Supporting Information.

Table S1. Parameters of the microwave-assisted hydrothermal synthesis and unit cell parameters of the $Na_3V_2O_{2x}(PO_4)_2F_{3-2x}$ solid solutions.

#	Reducing agent	Precursor load, mol $V_2O_5/NH_4H_2PO_4/NaF$	Reducing agent load, mol	Time, min	Temperature, °C	*a*, Å	*c*, Å	V, Å^3
1	$C_2H_2O_4$	0.004/0.008/0.012	0.008	15	180	6.3935(3)	10.6390(7)	434.88(3)
2	$C_2H_2O_4$	0.004/0.008/0.012	0.008	30	180	6.3932(2)	10.6345(6)	434.67(2)
3	$C_2H_2O_4$	0.004/0.008/0.012	0.008	30	200	6.3915(3)	10.6316(5)	434.32(4)
4	$C_2H_2O_4$	0.005/0.010/0.015	0.010	15	200	6.3915(2)	10.6289(5)	434.21(4)
5	$C_2H_2O_4$	0.005/0.010/0.015	0.010	6	220	6.3922(3)	10.6321(7)	434.44(6)
6	$C_2H_2O_4$*	0.0125/0.025/0.0375	0.025	15	200	6.3900(1)	10.6325(2)	434.15(1)
7	$C_6H_8O_7$	0.005/0.010/0.015	0.010	10	180	6.39585(7)	10.6355(2)	435.06(1)
8	$C_6H_8O_7$	0.005/0.010/0.015	0.010	30	180	6.3935(5)	10.628(1)	434.42(6)
9	$NaBH_4$	0.002/0.004/0.006	0.006	15	180	6.39189(9)	10.6331(2)	434.43(1)
10	$N_2H_4 \cdot H_2SO_4/C_2H_2O_4$	0.005/0.010/0.015	0.005/0.005	5	200	6.3891(13)	10.6404(3)	434.35(2)
11	$N_2H_4 \cdot HCl/C_2H_2O_4$	0.005/0.010/0.015	0.005/0.005	5	200	6.3929(2)	10.7014(4)	437.36(3)
12	$N_2H_4 \cdot HCl/C_2H_2O_4$	0.005/0.010/0.015	0.005/0.005	15	200	6.3964(1)	10.6989(4)	437.74(2)

* - the initial reagents were dissolved in 20 ml of deionized water

Table S2. Crystallographic data and Rietveld refinement parameters of the $Na_3V_2O_{2x}(PO_4)_2F_{3-2x}$ solid solutions.

Formula	$Na_3V_2O_2(PO_4)_2F$ (CSD 1904096)	$Na_3V_2O_{0.8}(PO_4)_2F_{2.2}$ (CSD 1904025)
Space group	*I*4/*mmm*	
a, Å	6.38643(4)	6.39455(5)
c, Å	10.62375(8)	10.6988(2)
V, Å^3	433.306(5)	437.475(11)
Z	2	2
ρ, г/см^3	3.16	3.15
Radiation	$CoK_{\alpha 1}$, λ = 1.78892 Å	$CuK_{\alpha 1}$, λ = 1.54056 Å
2θ, range, deg.	9.9 – 120	4 - 100
Number of reflections	71	87
Parameters refined	13	13
R_F, R_P, R_{wP}	0.036, 0.012, 0.016	0.032, 0.019, 0.024

Table S3. Atomic coordinates, occupancy factors and atomic displacement parameters for $Na_3V_2O_2(PO_4)_2F$ (first rows) and $Na_3V_2O_{0.8}(PO_4)_2F_{2.2}$ (second rows).

Atom	Position	Occupancy	*x/a*	*y/b*	*z/c*	U_{iso}, Å^2
Na1	8*h*	0.690(2)	0.2689(2)	*x*	0	0.0491(11)
		0.546(4)	0.2735(3)			0.0172(12)
Na2	16*l*	0.060(2)	0.195(5)	1/2	0	0.0491(11)
		0.102(2)	0.2105(15)	0.4043(15)		0.0172(12)
V1	4*e*	1	0	0	0.19950(10)	0.0243(5)
					0.19232(9)	0.0104(4)
P1	4*c*	1	0	1/2	1/4	0.0217(6)
						0.0043(5)
O1	16*n*	1	0	0.3082(2)	0.16305(12)	0.0164(4)
				0.30814(18)	0.16544(13)	0.0060(4)
O2	4*e*	1	0	0	0.3515(3)	0.0164(4)
		0.4O/0.6F*			0.3556(3)	0.0060(4)
F1	2*a*	1	0	0	0	0.0164(4)
						0.0060(4)

*- the occupancy factor was not refined.

Table S4. Main interatomic distances for $Na_3V_2O_2(PO_4)_2F$ and $Na_3V_2O_{0.8}(PO_4)_2F_{2.2}$.

$Na_3V_2O_2(PO_4)_2F$				$Na_3V_2O_{0.8}(PO_4)_2F_{2.2}$			
Na1-O1 ×4	2.4520(14)	V1–O1 ×4	2.0063 (13)	Na1-O1 ×4	2.4983(18)	V1 – O1 ×4	1.9909(12)
Na1-O2	2.616(2) ×2	V1 – O2	1.615(4)	Na1-O2	2.565(2) ×2	V1 – O2	1.748(3)
Na1-F1	2.4284(16)	V1 – F1	2.1194(10)	Na1-F1	2.473(2)	V1 – F1	2.0579(10)
		BVS = 4.052(16)				BVS = 3.395(7)	
Na2-O1	2.461(15) ×4			Na2-O1	2.311(6) ×2		
Na2-O2	2.51(1) ×2	P1 – O1 ×4	1.5340(13)	Na2-O1	2.886(8) ×2	P1 – O1 ×4	1.5242(12)
Na2-F1	2.76(2)			Na2-O2	2.483(8) ×2		
				Na2-F1	2.919(10)		

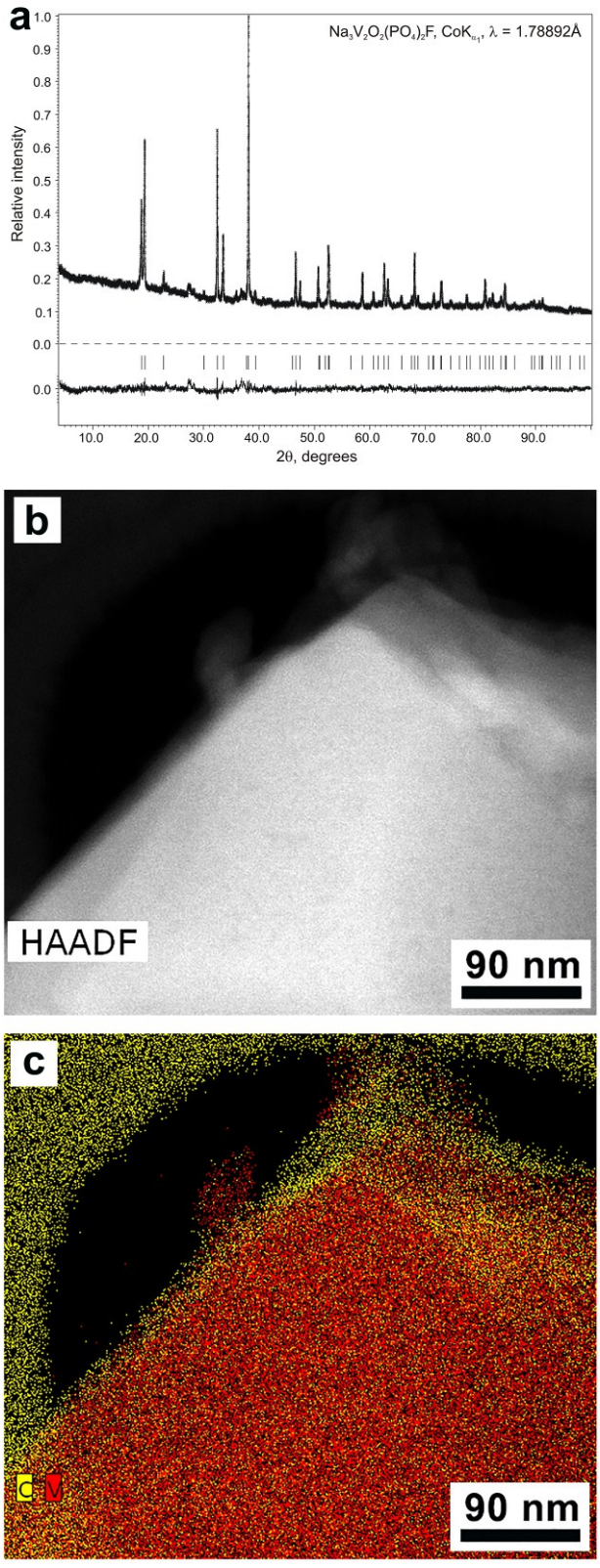

Fig. S1. The experimental, calculated and difference PXRD profiles for $Na_3V_2O_2(PO_4)_2F$ carbon-coated with dopamine and annealed at 600 °C for 3 h after Rietveld refinement (a); EDX mapping (carbon and vanadium) for $Na_3V_2O_2(PO_4)_2F$ carbon-coated by dopamine and annealed at 600 °C for 3 h (b, c).

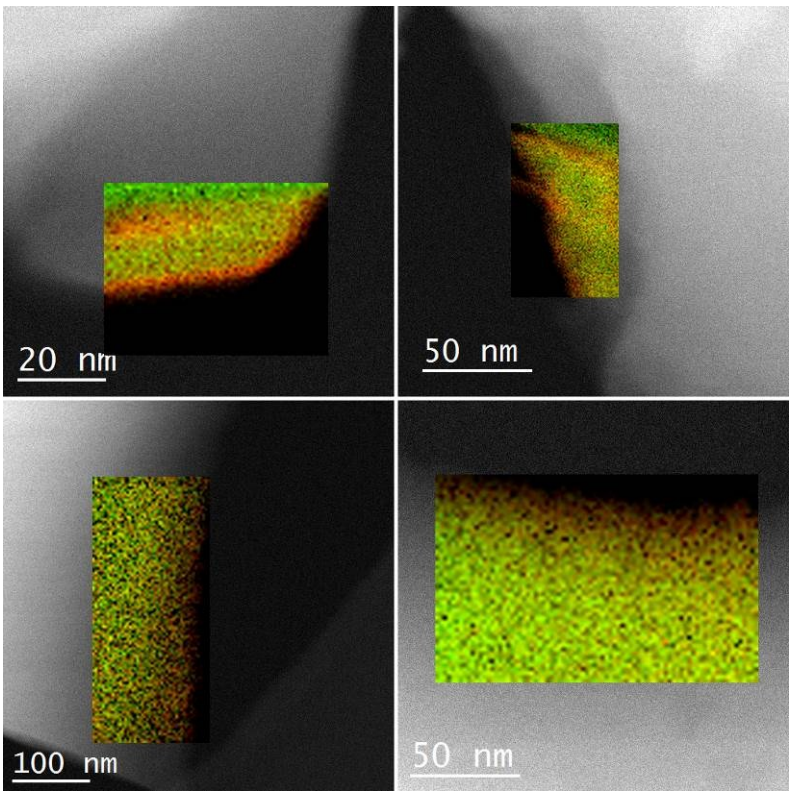

Fig. S2. STEM-EELS mapping of V^{3+} (red) and V^{4+} (green) at the surface of the crystallites in $Na_3V_2O_2(PO_4)_2F$ synthesized with oxalic acid. The V^{3+} and V^{4+} signals were integrated within 1 eV windows centered at 517.8 eV and 519.2 eV, respectively.

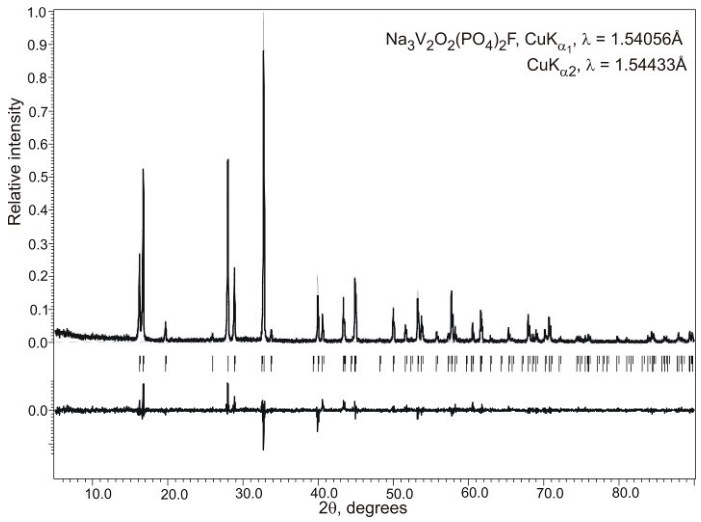

Fig. S3. The experimental, calculated and difference PXRD profiles for the 3 g batch of $Na_3V_2O_2(PO_4)_2F$ after Rietveld refinement.

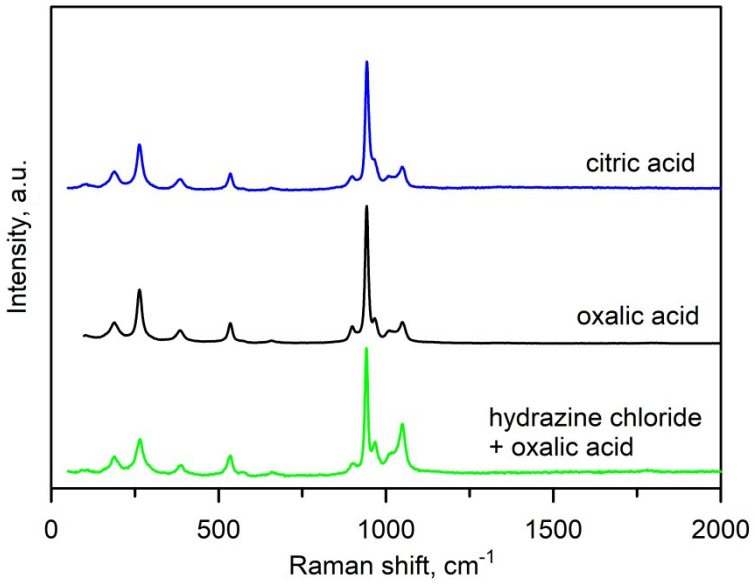

Fig. S4. Raman spectra of $Na_3V_2O_2(PO_4)_2F$ prepared with citric acid (blue) and oxalic acid (black) and the spectrum of $Na_3V_2O_{0.8}(PO_4)_2F_{2.2}$ synthesized with the mixture of hydrazine chloride with oxalic acid (green).

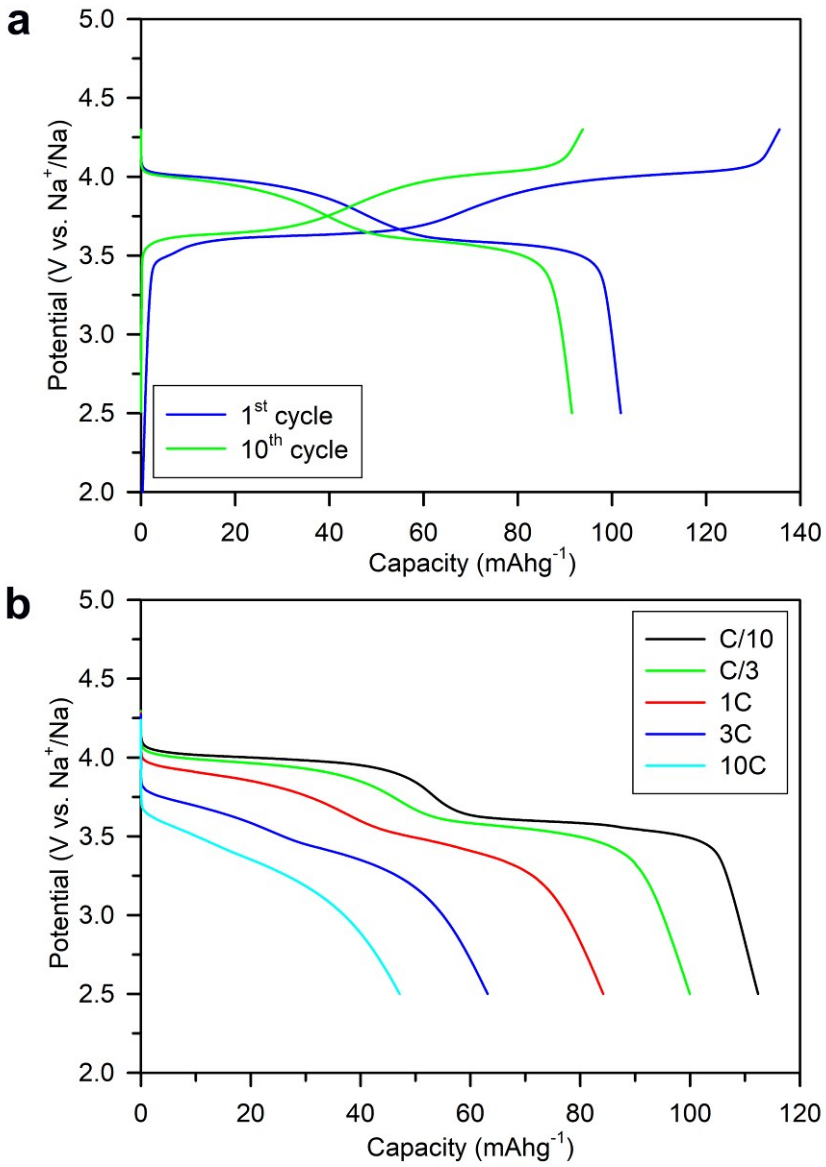

Fig. S5. Electrochemical performance of $Na_3V_2O_2(PO_4)_2F$ obtained with citric acid as a reducing agent, in the potential range 2.5÷4.3 V rel. Na^+/Na, at room temperature: galvanostatic charge-discharge profiles of 1st and 10th cycles after cycling at C/10 current density (a); galvanostatic charge-discharge profiles at different current densities (b).

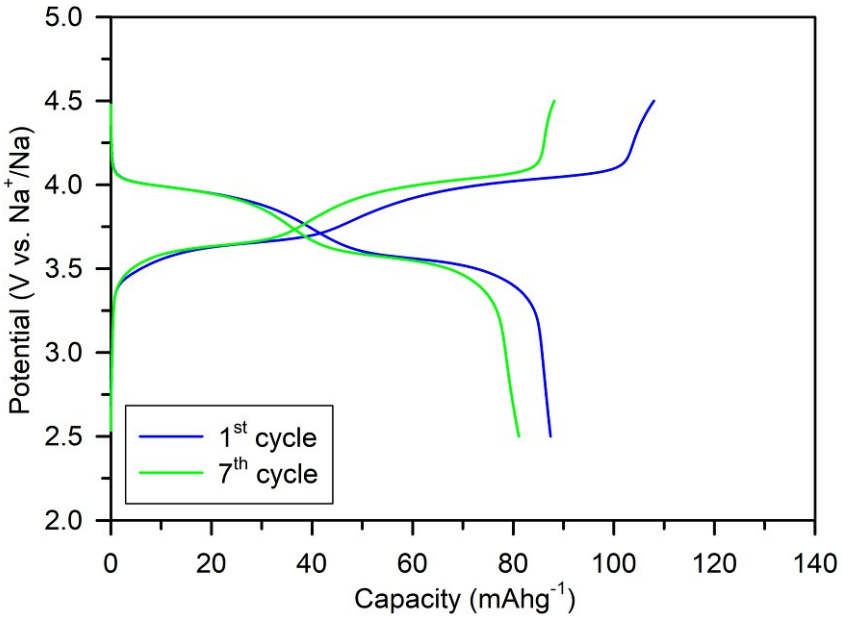

Fig. S6. Electrochemical performance of $Na_3V_2O_2(PO_4)_2F$ obtained with $NaBH_4$ as a reducing agent, in the potential range 2.5÷4.5 V rel. Na^+/Na, at room temperature: galvanostatic charge-discharge profiles of 1st and 7th cycles after cycling at C/10 current density

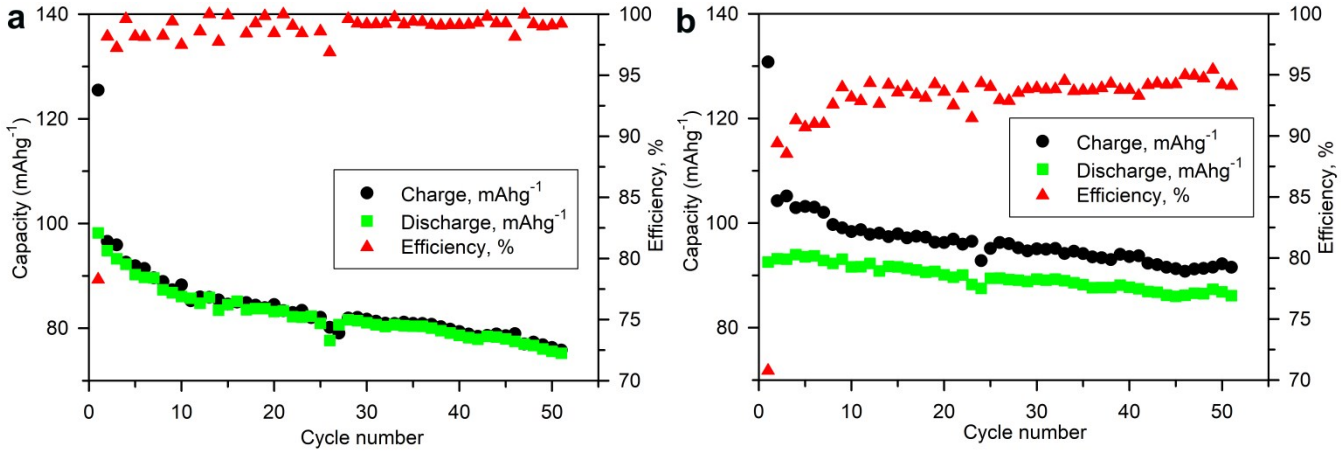

Fig. S7. Coulombic efficiency of $Na_3V_2O_2(PO_4)_2F$ annealed with glucose (8 mass. %) at 600°C during 1 h (a), coated with dopamine for 24 h and annealed at 500°C during 3 h (b) in the potential range 2.5÷4.3 V vs. Na^+/Na at room temperature cycled at C/2 current densities.

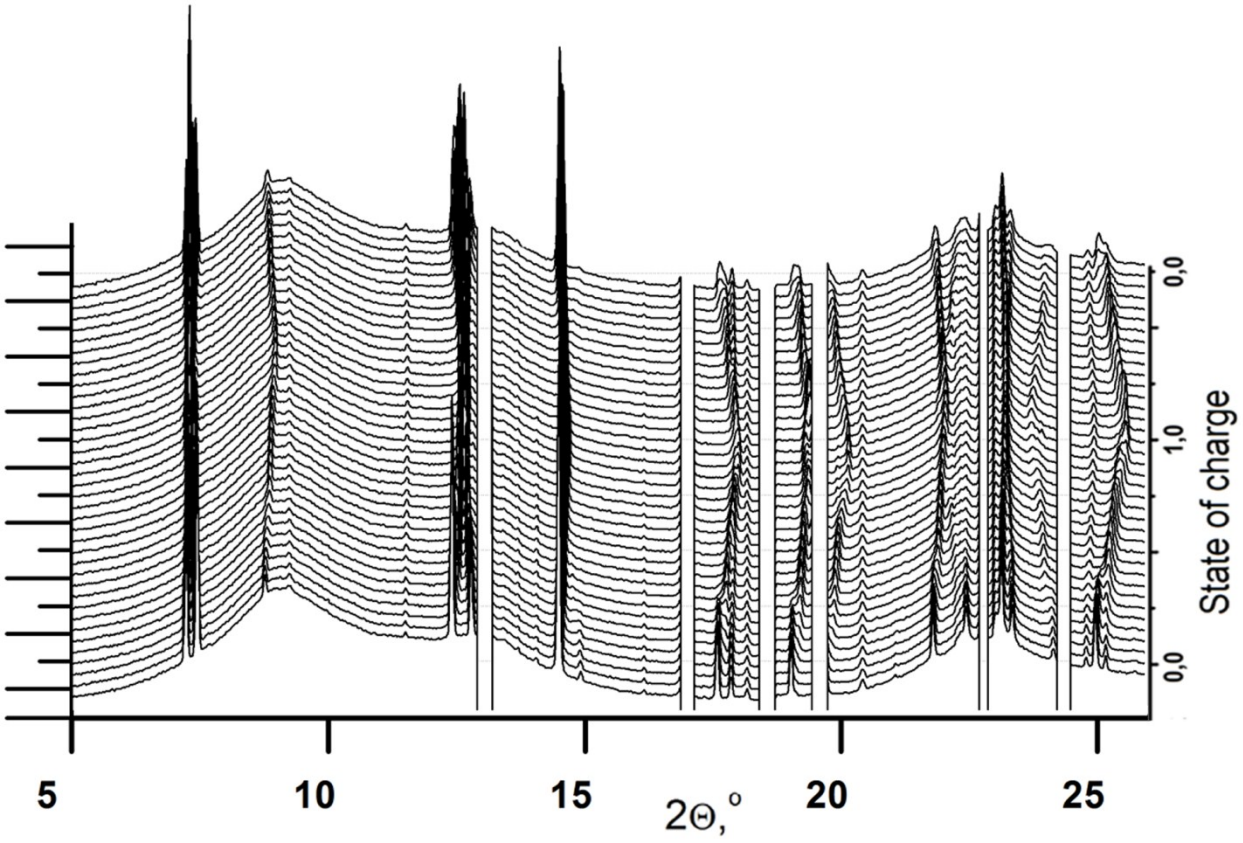

Fig. S8. Extended (5-26° 2θ) range of SXPD patterns collected in *operando* regime. Deleted regions contain Al and Na reflections